
REPORT No. 267

DRAG OF WINGS WITH END PLATES

By PAUL E. HEMKE
Langley Memorial Aeronautical Laboratory

REPORT No. 267

DRAG OF WINGS WITH END PLATES

By PAUL E. HEMKE

SUMMARY

In this report a formula for calculating the induced drag of multiplanes with end plates is derived. The frictional drag of the end plates is also calculated approximately. It is shown that the reduction of the induced drag, when end plates are used, is sufficiently large to increase the efficiency of the wing.

Curves showing the reduction of drag for monoplanes and biplanes are constructed; the influence of gap-chord ratio, aspect ratio, and height of end plate are determined for typical cases. The method of obtaining the reduction of drag for a multiplane is described.

Comparisons are made of calculated and experimental results obtained in wind tunnel tests with airfoils of various aspect ratios and end plates of various sizes. The agreement between calculated and experimental results is good.

Analysis of the experimental results shows that the shape and section of the end plates are important.

INTRODUCTION

The end plates which are dealt with in this report are fins or shields which are attached to the tips of airfoils; the plane of the fin is perpendicular to the span of the airfoil. The purpose of this device is to serve as a barrier to the flow along the span and around the tips of the airfoil. This flow in a vertical plane containing the span is usually called the transverse flow. By obstructing this transverse flow its kinetic energy is diminished and as a consequence the induced drag of the airfoil is thereby reduced.

From wind tunnel tests made at Göttingen (Reference 1) and at the Langley Memorial Aeronautical Laboratory (Reference 2), it has been learned that the induced drag may be materially reduced by the use of end plates. The reduction of the induced drag exceeds the additional frictional drag of the end plates which were used in these tests for all but small values of the lift coefficients.

The German tests were analyzed but the method of analysis gives no direct information on the value of the frictional drag of the end plates. The American tests have not been previously analyzed.

In this report a formula for calculating the induced drag of multiplanes with end plates is derived. The induced drag is calculated by finding the kinetic energy of the transverse flow using the method of conformal transformation. The induced drags of the monoplane and biplane with end plates are found as special cases of this general formula.

The formula for the monoplane is used to calculate the reductions of drag for the airfoils tested at Göttingen and the Langley Memorial Aeronautical Laboratory. Comparison of calculated and experimental results for airfoils of various aspect ratios with end plates of various sizes are made. Curves illustrating the total reduction of drag for monoplanes and biplanes are constructed; the influence of such major factors as gap-chord ratio, aspect ratio, and height of end plates is determined. In all cases the frictional drag of the end plates is considered in calculating the total drag.

INDUCED DRAG OF A MULTIPLANE WITH END PLATES

The longitudinal projection of the multiplane consists of equal, parallel straight lines. The same projection of the end plates will also be considered as straight lines whose directions are at right angles to the projection of the multiplane elements.

The induced angle of attack and consequently the induced drag depend upon the induced downwash. It is sufficient then for the purpose in hand to consider the transverse flow in a vertical plane at right angles to the air stream.

This two-dimensional transverse flow may be determined in several ways. In this report it has been obtained by using the method of conformal transformation. The rectilinear polygon bounding the longitudinal projection of the wings and end plates is transformed into a single straight line. The flow around such a line is well known.

Let the plane of the lines with end pieces be the plane of a complex variable z as shown in Figure 1. The mid-point of the system of lines is at the origin and the direction of the lines

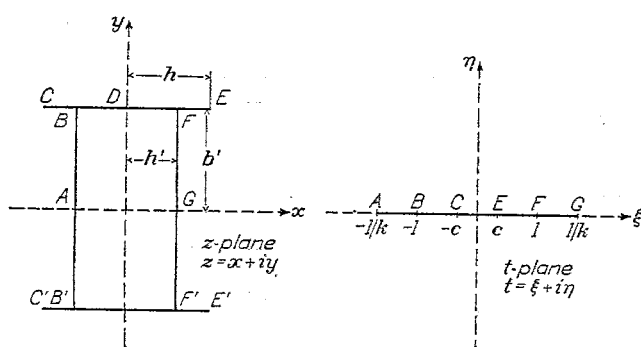


FIG. 1.—Conformal representation of biplane with end plates

coincides with that of the axis of imaginaries. The end pieces CE and C'E' are then parallel to the real axis and are each of length $2h$. The bounding rectangle BFF'B' has dimensions $2b' \times 2h'$. It is assumed that $h \leq h'$.

The transformation to an auxiliary t -plane is effected by means of the theorem usually called the Schwarz-Christoffel theorem. According to this theorem, if $z = x + iy$ and $t = \xi + i\eta$ then any polygon bounded by straight lines in the z -plane can be transformed into

the axis of ξ , points inside the polygon corresponding to points on one side of the axis of ξ . The transformation is

$$\frac{dz}{dt} = A(t - \xi_1)^{\frac{\alpha_1 - 1}{\pi}} (t - \xi_2)^{\frac{\alpha_2 - 1}{\pi}} \cdots (t - \xi_n)^{\frac{\alpha_n - 1}{\pi}} \quad (1)$$

where $\alpha_1, \alpha_2, \dots, \alpha_n$ are internal angles of the polygon in the z -plane and $\xi_1, \xi_2, \dots, \xi_n$ are the points on the axis of ξ that correspond to the angular points of the polygon in the z -plane and A is a real constant.

In our application we shall consider the polygon $-\infty A B C D E F + \infty$ in the z -plane as transformed into the upper half of the t -plane. By the theory if the point $\xi = \infty$ be taken to correspond with one corner of the polygon the corresponding factor in the expression for dz/dt is omitted. Also we may choose three values of ξ arbitrarily since a polygon similar to a given polygon of n sides may be constructed by means of $n - 3$ relations between the sides.

We shall accordingly choose the three points as follows:

	D	F	∞
z	ib'	$h' + ib'$	∞
t	0	1	∞

Then to the points E and G will correspond the values $\xi = c$ and $\xi = \frac{1}{k}$, respectively. The transformation is then found in the form

$$\frac{dz}{dt} = a \frac{(t^2 - c^2)}{\sqrt{(t^2 - 1) \left(t^2 - \frac{1}{k^2} \right)}}, \quad (2)$$

where a is a real constant.

We may integrate (2) by substituting $t = sn \omega \pmod{k}$. $sn \omega$ denotes an elliptic function and from the relations given in textbooks on these functions we find,

$$z = \frac{a}{k} \left[Z(\omega) - \omega \left(1 - \frac{E}{K} - k^2 c^2 \right) \right] + \beta \quad (3)$$

Here $Z(\omega)$ is Jacobi's zeta-function.

The correspondence between the various points is exhibited in the following table:

A	B	C	D	E	F	G	∞
$z, -h'$,	$-h' + ib'$,	$-h + ib'$,	ib' ,	$h + ib'$,	$h' + ib'$,	h' ,	∞
$t, -1/k$,	-1 ,	$-c$,	0 ,	c ,	1 ,	$1/k$,	∞
$\omega, -K + iK'$,	$-K$,	$-\omega_0$	0 ,	ω_0 ,	K ,	$K + iK'$,	iK'

K and E are the complete elliptic integrals of the first and second kind, K' being the complete elliptic integral of the first kind for the comodulus k' ($k'^2 = 1 - k^2$).

Since $c = sn \omega_0$ we may now use the relation $1 - \frac{E}{K} - k^2 sn^2 \omega_0 = Z'(\omega_0)$. This relation is also found in textbooks on elliptic functions. The prime accent indicates differentiation with respect to the variable ω . We then have

$$z = \frac{a}{k} [-\omega Z'(\omega_0) + Z(\omega)] + \beta, \quad a \text{ and } \beta \text{ constants.} \quad (4)$$

Using (4) and the correspondence given in the table we have the following equations:

$$\frac{a}{k} [-\omega_0 Z'(\omega_0) + Z(\omega_0)] + \beta = h + ib' \quad (5)$$

$$\frac{a}{k} [-K Z'(\omega_0)] + \beta = h' + ib' \quad (6)$$

$$\frac{a}{k} [-(K + iK') Z'(\omega_0)] - \frac{i\pi}{2K} + \beta = h' \quad (7)$$

Solving these we have:

$$h = \frac{a}{k} [Z(\omega_0) - \omega_0 Z'(\omega_0)]; \quad ib' = \beta$$

$$h' = -\frac{a}{k} [K Z'(\omega_0)]$$

$$b' = \frac{a}{k} \left[K' Z'(\omega_0) + \frac{\pi}{2K} \right]$$

$$\frac{h}{b'} = \frac{Z(\omega_0) - \omega_0 Z'(\omega_0)}{K' Z'(\omega_0) + \frac{\pi}{2K}} \quad (8)$$

$$\frac{h'}{b'} = \frac{-K Z'(\omega_0)}{K' Z'(\omega_0) + \frac{\pi}{2K}} \quad (9)$$

If $\frac{h'}{b'} = \gamma, \quad Z'(\omega_0) = \frac{-\pi\gamma}{2K(K + \gamma K')} \quad (10)$

$$\frac{a}{k} = \frac{2b'(K + \gamma K')}{\pi} \quad (11)$$

$$z = b' \left[\frac{2(K + \gamma K')}{\pi} Z(\omega) + \frac{\omega b' \gamma}{K} + i \right] \quad (12)$$

The transverse flow around the lines with end pieces is parallel to the real axis at infinity in the z -plane, the direction of flow at infinity being in the direction of the positive x -axis. The potential function for this flow is more easily expressed in terms of t . It is $\Phi_i = \varphi_i + i\psi_i = \alpha Vt$, where V is the velocity of the flow in the z -plane at a great distance from the origin.

If we superimpose on this flow one whose potential function is $\Phi_s = -Vz$ we shall have the potential function for the flow set up by the motion of the lines in a fluid otherwise at rest. The lines will move in the direction of the positive real axis in the z -plane with a constant velocity V .

To find the kinetic energy we evaluate the integral

$$-\frac{1}{2} \rho \int_L \varphi \frac{\partial \varphi}{\partial n} ds \quad (\text{Reference 3, p. 44}).$$

The path of integration, L , is the complete boundary of the wing, φ is the real part of $(\alpha Vt - Vz)$, $\frac{\partial \varphi}{\partial n}$ is the normal velocity component along the boundary and ds is the element of length of the boundary. We have

$$T = 2\rho V^2 \alpha^2 \frac{\pi}{2} \left[\frac{1}{2} \left(1 + \frac{1}{k^2} \right) - c^2 \right]$$

By using again the relation $1 - \frac{E}{K} - k^2 c^2 = Z'$ (ω_0) as well as equations (10) and (11), we have

$$T = \frac{1}{2} \rho V^2 \frac{4b'^2 (K + K'\gamma)^2}{\pi} \left[\frac{2E}{K} - k'^2 - \frac{\pi\gamma}{K(K + \gamma K')} \right] \quad (13)$$

This may be written $T = \frac{1}{2} \rho V^2 A_M$ where

$$A_M = \frac{4b'^2 (K + K'\gamma)^2}{\pi} \left[2 \frac{E}{K} - k'^2 - \frac{\pi\gamma}{K(K + K'\gamma)} \right] \quad (14)$$

Prandtl (Reference 4, p. 48) has shown that, if it is assumed that all air particles within an air stream of cross sectional area A_M are uniformly deflected downward by the wing and all outside are not deflected, then the correct lift and the correct work due to the induced drag are obtained by application of the impulse theorem and the energy theorem. Doctor Zahm has suggested that A_M be called the *area of the equivalent air stream* and this term will be used throughout the report.

As the minimum induced drag of the wing system is known to be $D_i = \frac{L^2}{4q A_M}$, where L is the lift and q the dynamic pressure, it may be computed by using equation (14).

THE MONOPLANE WITH END PLATES

The area of the equivalent air stream of the monoplane with end plates is found from (14) by setting $\gamma = 0$.

$$A_M = \frac{4b'^2 K^2}{\pi} \left(\frac{2E}{K} - k'^2 \right)$$

If the span is b we have

$$A_M = \frac{K^2 b^2}{\pi} \left[\frac{2E}{K} - k'^2 \right] \quad (15)$$

This reduces when $b' = b = 0$ to

$$A_M = \frac{\pi b^2}{4} \text{ which is known to be correct.}$$

The ratio of the area of the equivalent air stream of the monoplane to that of the monoplane with end plates is

$$R = \frac{\pi^2}{4K^2 \left(\frac{2E}{K} - k'^2 \right)} \quad (16)$$

Values of R were calculated in the following manner: When $\gamma=0$, $Z'(\omega_0)=0$, and ω_0 was then found from a table of elliptic functions (Reference 5) after the modulus k had been arbitrarily assigned. k is usually expressed as the sine of a modular angle, θ . Then $2h/b$ and R were calculated using equations (8) and (16).

Table I contains the values of R for various values of $2h/b$. The quantity J as given by Nagel (Reference 2) is related to R by the equation

$$R = \frac{\pi}{8J}$$

The value of R obtained by using the approximate formula

$$J = \frac{\pi}{8} + 0.6515 \left(\frac{2h}{b} \right) \text{ is also given in Table I.}$$

Let us consider now an airfoil whose span is b and chord c . We shall assume that the longitudinal projection of the airfoil is a straight line. The width of the end plate is taken as a chord length where no statement to the contrary is made. The coefficient of minimum induced drag is then

$$C_{Di} = \frac{C_L^2 S}{4\pi A_M}$$

$$C_L = \text{lift coefficient}$$

$$S = \text{area of wing.}$$

Using (16) this may be written

$$C_{Di} = \frac{C_L^2 R S}{\pi b^2} \quad (17)$$

The use of end plates introduces an additional frictional drag. This frictional drag may be designated D_F and is given by

$$D_F = C_F q S'$$

The end plates act as airfoils so that C_F is a drag coefficient and S' is the area of the two end plates.

The difference of total drag coefficient, C_D , and profile drag coefficient, C_{DP} , is

$$C_D - C_{DP} = \frac{C_L^2 R S}{\pi b^2} + C_F \frac{S'}{S}$$

The same expression for a wing without end plates is $\frac{C_L^2 S}{\pi b^2}$. To determine the actual gain with a given set of end plates we subtract these two expressions. If we call this difference ΔC_D , we have

$$\Delta C_D = \frac{C_L^2 S}{\pi b^2} (1 - R) - C_F \frac{S'}{S} \quad (18)$$

If the width of the end plate is a chord length and the height $2h$, then

$$\frac{S'}{S} = \frac{4ch}{cb} = \frac{4h}{b}$$

Then

$$\Delta C_D = \frac{C_L^2 S}{\pi b^2} (1 - R) - 2C_F \left(\frac{2h}{b} \right) \quad (19)$$

If we use

$$R = \frac{\pi}{8J} = \frac{1}{1 + 1.66 \left(\frac{2h}{b} \right)},$$

we have

$$\Delta C_D = \frac{C_L^2 S}{\pi b^2} \frac{1.66 \left(\frac{2h}{b} \right)}{1 + 1.66 \left(\frac{2h}{b} \right)} - 2C_F \left(\frac{2h}{b} \right) \quad (20)$$

From this the reduction of drag for a given end plate may be easily found. Figure 2 shows parabolas obtained from (20) by using a fixed value of b^2/S , C_F , and different sizes of end plates. For smaller values of b^2/S the slopes of the parabolas increase but the intersection points on the vertical axis are not altered. There is consequently a greater average reduction of drag for the smaller values of b^2/S over the usual range of values of the lift coefficient.

ANALYSIS OF WIND TUNNEL RESULTS

The Göttingen tests (Reference 1) were made with single airfoils. The end plates were flat and of various shapes and sizes. Two aspect ratios were used, 8/3 and 4/3. In the analysis made of these tests the frictional drag of the end plates was not actually calculated. In this report this quantity has been calculated approximately.

Figures 3, 4, and 5 show the results of the Göttingen tests, for aspect ratio 8/3, in the form of polar curves. In each case except for end plate 3, Figure 4, the reduction of drag was computed from formula (19) using the appropriate value of aspect ratio, ratio of length of end plate to span and area of end plates. In the case of end plate 3, since the end of the wing was only partially shielded, an average height of the plate, over the chord, was used. The value of C_F which gave the best agreement for the frictional drag of the end plates is 0.0140.

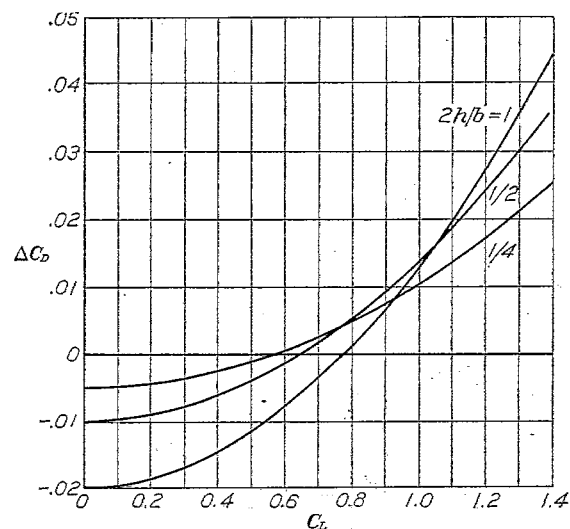


FIG. 2.—Monoplane with end plates. Calculated reduction of drag, ΔC_D , against lift coefficient for various values of $2h/b$. $2h$ = height of end plate. b = span. Aspect ratio, 6. Drag coefficient, $C_F = 0.01$

This calculated reduction of drag was then laid off on each diagram starting from the polar obtained when using the wing without end plates. Unfortunately, no tabular values of drag and lift coefficients were given in the Göttingen report. Consequently, no accurate comparisons of calculated and observed reduction of drag could be made.

On the whole, the agreement between calculated and observed reductions of drag is good for that portion of the polar curve where the angles of attack are smaller than the burbling angle. The use of a partial end plate such as end plate 3 is not satisfactory. In this instance the disturbance of flow around the end of the wing apparently increases the frictional drag at low values of C_L and the reduction of drag is not as great at the higher values of C_L .

The American tests (Reference 2) were made at the Langley Memorial Aeronautical

Laboratory. Single airfoils, wing section N. A. C. A. 73, with aspect ratio 6 were used in these tests. Only two plates, one circular, the other trapezoidal, were tried. These plates were streamlined and consequently the value of C_F to be used in making the calculations is different. The value 0.008 (Reference 1) proved satisfactory.

The results of these tests are shown graphically in Figures 6 and 7. The reduction of drag was calculated as before, C_F only being changed in value. Since tabular values are available much closer comparison could be made. The calculated and observed reductions of drag are shown in tabular form in Table II, and graphically in Figures 6, 7, and 8. The agreement is good, considering that we have only an approximation to the actual reduction in consequence of the simplifying assumptions made in the calculations.

Comparing the two series of tests we see that theory and experiment show a larger reduction of drag for smaller aspect ratios. The use of end plates with good aerodynamical profile sections is preferable since this reduces the drag for all values of C_L . This is illustrated by the two series of tests studied; in one the coefficient is 0.014, and in the other 0.008.

The agreement between calculated and observed reductions of drag in the American tests suggests using an end plate of given area in the best possible way. Since the use of the entire height of the trapezoidal end plate (fig. 6) in the formula gave calculated results agreeing very

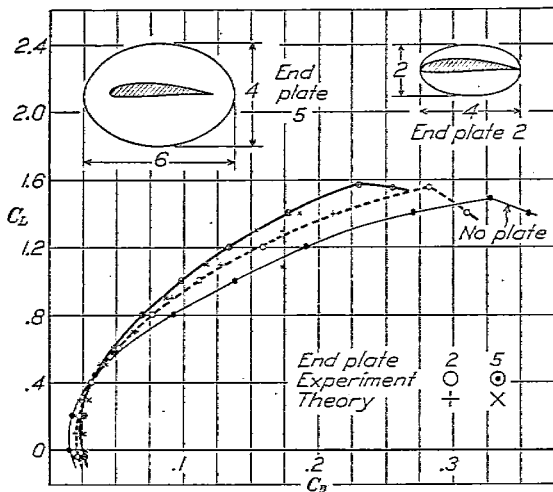


FIG. 3.—Polar curves of Göttingen tests showing reduction of drag due to end plates 2 and 3. Aspect ratio 8/3

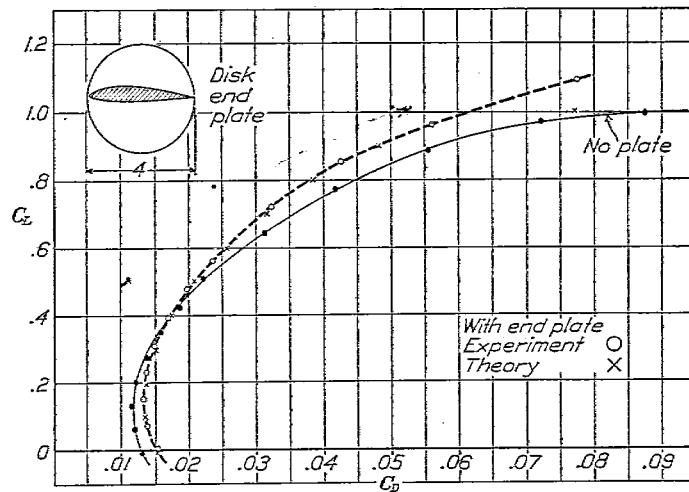


FIG. 6.—Polar curves of N. A. C. A. tests showing reductions of drag due to disk end plates. N. A. C. A. 73 airfoil. Aspect ratio, 6

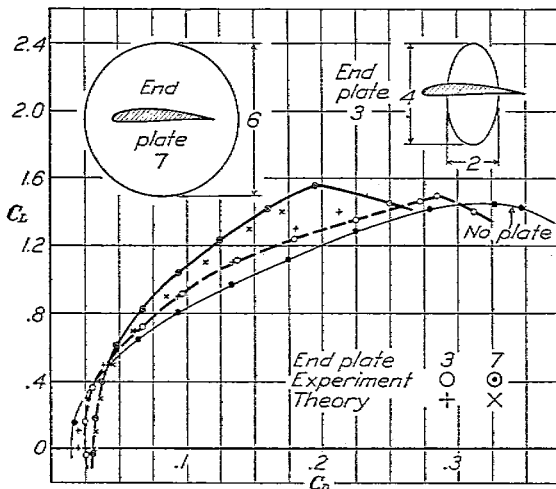


FIG. 4.—Polar curves of Göttingen tests showing reduction of drag due to end plates 3 and 7. Aspect ratio, 8/3

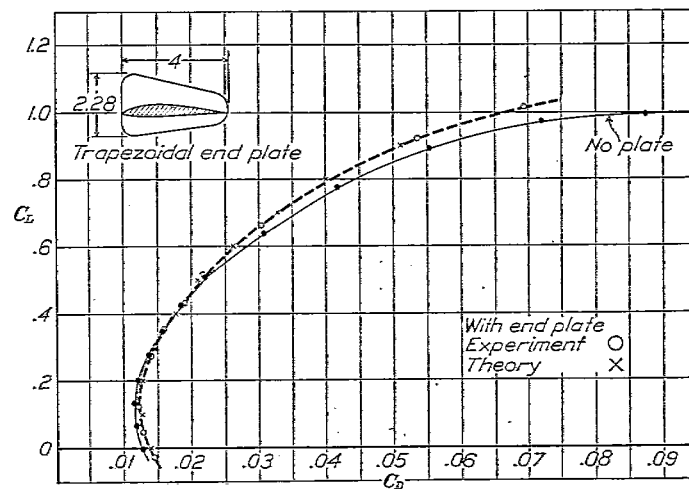


FIG. 7.—Polar curves of N. A. C. A. tests showing reductions of drag due to trapezoidal end plates. N. A. C. A. 73 airfoil. Aspect ratio, 6

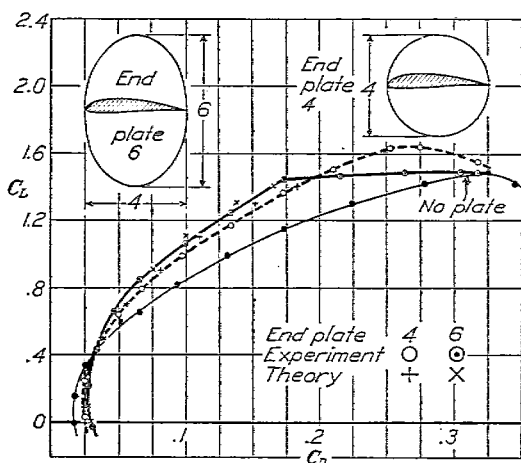


FIG. 5.—Polar curves of Göttingen tests showing reduction of drag due to end plates 4 and 6. Aspect ratio, 8/3

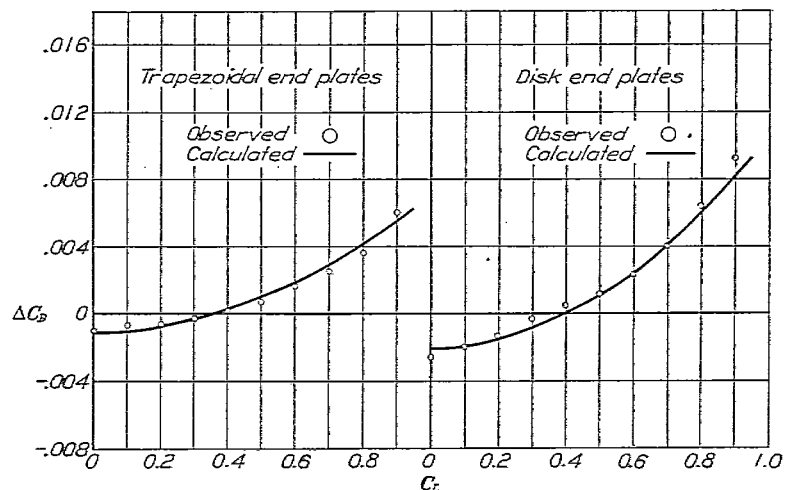


FIG. 8.—Calculated and observed differences of drag of wings with different end plates. N. A. C. A. 73 airfoil. Aspect ratio, 6

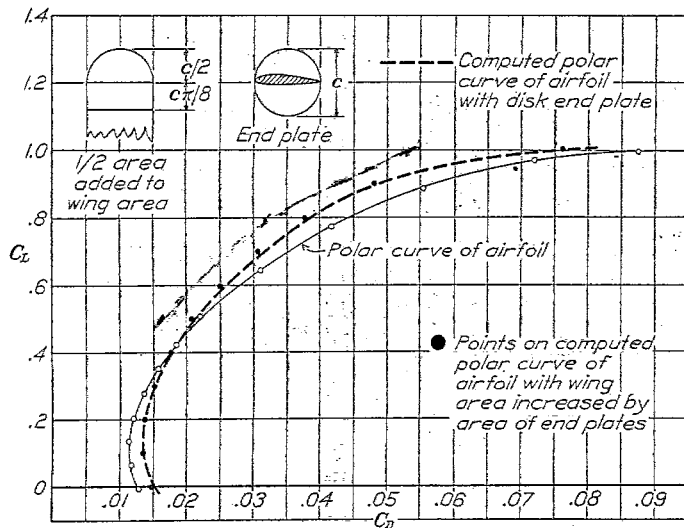


FIG. 9.—Calculated reduction of drag using disk end plates and increasing wing area by an amount equal to area of end plates. N. A. C. A. 73 airfoil. Aspect ratio, 6

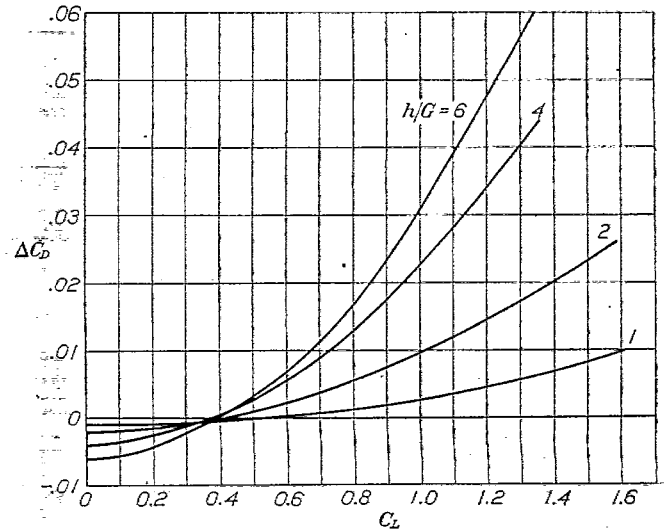


FIG. 11.—Biplanes with end plates. Calculated reduction of drag, ΔC_D , plotted against lift coefficient for various values of h/G . $2h$ = height of end plate. $2G$ = gap. Span/chord = 6. Gap/chord = 1.00. Drag coefficient, $C_F = 0.01$

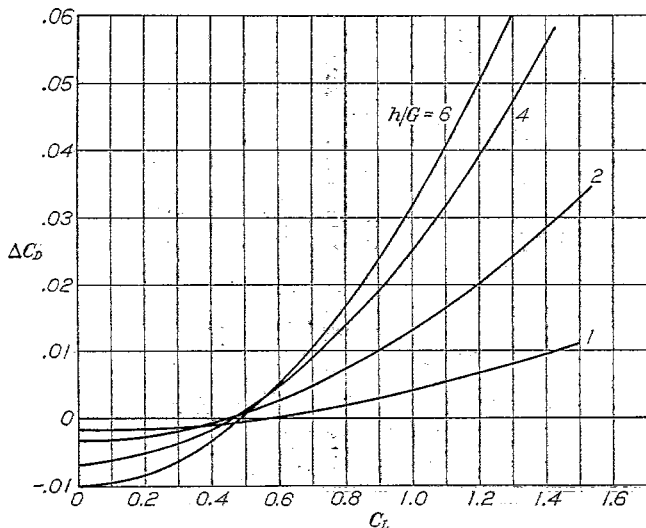


FIG. 10.—Biplanes with end plates. Calculated reduction of drag, ΔC_D , plotted against lift coefficient for various values of h/G . $2h$ = height of end plate. $2G$ = gap. Span/chord = 6. Gap/chord = 0.6. Drag coefficient, $C_F = 0.01$

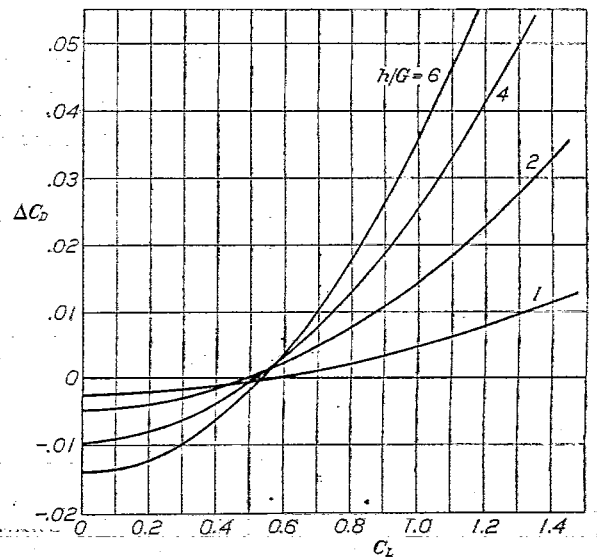


FIG. 12.—Biplanes with end plates. Calculated reduction of drag, ΔC_D , plotted against lift coefficient for various values of h/G . $2h$ = height of end plate. $2G$ = gap. Span/chord = 6. Gap/chord = 1.40. Drag coefficient, $C_F = 0.01$

well with observed results, it appears that an end plate of a given area, and therefore having a fixed frictional drag, may have a greater effect on the drag in one shape than in another. In particular, the tests and calculations with this end plate make it seem plausible that the greater part of the restriction of the transverse flow occurs over the forward portion of the span and that a shape which has greater height in the portion nearer the leading edge is advantageous to use.

Nagel (Reference 1) has stated that the reduction of drag when using end plates, does not equal the corresponding reduction obtained when the span is increased by an amount equal to the sum of the heights of the end plates. The reason for adding to the span an amount equal to the total height of end plates is not quite evident. The addition to the span might also be made, with as good reason, by adding to the wing area the sum of the areas of the two end plates. Such a comparison is shown graphically in Figure 9. The polar curve of an airfoil is shown compared with the computed polar curves when end plates are added to the wing and

when the wing area is increased by an amount equal to the total area of the end plates. The comparison was made using the same drag coefficient for the end plates as for the additional wing area. The results do not differ much.

CALCULATED REDUCTION OF DRAG FOR MULTIPLANES WITH END PLATES

The method will be used to calculate first the reduction of drag for a biplane. The area of the equivalent air stream for a biplane with end plates is given by equation (14). The end plates must have heights equal to or greater than the gap of the biplane, for otherwise the flow would change to such an extent that (14) would no longer hold. This formula reduces when $h = h'$, that is, when the end plate has a height equal to the gap of the biplane, to one which has been previously derived (Reference 6). It is evident from the correspondence of values between z , t and ω that when

$$h = h', \quad \omega_0 = K, \quad Z(\omega_0) = 0 \quad \text{and} \quad Z'(\omega_0) = 1 - \frac{E}{K} - k^2.$$

From (10) we find then

$$\gamma = \frac{E - K k'^2}{E' - K' k^2} \quad \text{and} \quad A_M = \pi b^2 \cdot \frac{k'^2}{E' - k^2 K'}.$$

For a span b this reduces to

$$A_M = \frac{\pi b^2}{4} \cdot \frac{k'^2}{E' - k^2 K'}$$

which is the value previously found.

The expression for reduction of drag is derived in a manner quite similar to that used for the monoplane. We find

$$\Delta C_D = \frac{C_L^2}{2} \left(\frac{c}{b} \right) \left(\frac{b^2}{A_M} - \frac{b^2}{A_{M_1}} \right) - C_F \left(\frac{2h}{b} \right).$$

b = span of biplane.

c = chord.

C_L = lift coefficient.

A_M = area of the equivalent air stream of a biplane without end plates.

A_{M_1} = area of the equivalent air stream of a biplane with end plates.

C_F = drag coefficient of end plates.

$2h$ = height of end plate (width assumed to be c).

If we introduce Prandtl's ratio $x = \frac{\pi b^2}{4 A_M}$ and a similar ratio

$$x_1 = \frac{\pi b^2}{4 A_{M_1}} \quad \text{we have}$$

$$\Delta C_D = \frac{2 C_L^2 c}{\pi b} (x - x_1) - C_F \left(\frac{2h}{b} \right) \quad (22)$$

The value of x_1 depends on both the gap/chord ratio and the ratio of height of end plate to gap. The former ratio is γ and has been chosen in each calculation. The calculations were made in the following manner:

- (a) $Z'(\omega_0)$ was found from $Z'(\omega_0) = \frac{\pi \gamma}{2 K (K + \gamma K')}$, after γ has been arbitrarily assigned.
- (b) From $dn^s \omega_0 = \frac{E}{K} + Z'(\omega_0)$, ω_0 was found using the table of elliptic functions (Reference 4).
- (c) The value of $\frac{2h}{b} = \frac{Z(\omega_0) - \omega_0 Z'(\omega_0)}{\frac{\pi}{2K} + K' Z'(\omega_0)}$ was calculated next.
- (d) $A_{M_1} = \frac{b^2 (K + K' \gamma)^2}{\pi} \left[2 \frac{E}{K} - k'^2 - 2 Z'(\omega_0) \right]$ was evaluated then quite easily.

Figures 10, 11, and 12 show the calculated reductions of drag for span/chord of 6 and gap/chords of 0.6, 1.0, and 1.4. In each case the following values of h/h' were used; $h/h' = 1, 2, 4, 6$ and, as in Figure 2, the value $C_F = .01$ was used as it represents an average value of C_F .

The curves illustrate how properties of end plates affect biplanes of various proportions. The increase of drag at lower values of C_L is considerably less than it is for larger values of gap/chord while the reduction of drag, especially when larger plates are used, is relatively large.

The reduction of drag persists at the higher values of C_L for plates which are quite large, so large as to be useless in practice.

The method used in calculating the effect of end plates for biplanes may be used for multiplanes. Formula (22) would differ only as far as x is concerned. This quantity may be calculated, however (Reference 7), and the reductions of drag for multiplanes may be calculated in precisely the same manner as that just described and carried out for biplanes.

CONCLUSIONS

Calculations show that the induced drag of monoplanes and multiplanes may be decreased by attaching end plates to the ends of the wing. The frictional drag of the end plates may be calculated approximately. The reduction of the induced drag exceeds the additional frictional drag due to the end plates at all but small values of the lift. For given dimensions of wings and end plates the reduction of drag less the frictional drag of the end plates varies directly as the square of the absolute lift coefficient. The average reduction of drag increases as the aspect ratio decreases. Calculations and experiments agree quite satisfactorily for single wings equipped with end plates.

Wind tunnel tests show that the coefficient used in calculating the frictional drag of the end plates may be reduced materially by fairing the end plates. The shape of the end plate determines to some extent the reduction of induced drag. Further tests would be necessary to find end plates of good shape and having at the same time a low drag coefficient.

Recent experiments have shown that much higher lift coefficients can be obtained than has been the case up to now with the conventional airfoils. Since the reduction of drag due to end plates is much greater at the higher values of the lift coefficient, the use of end plates together with the use of means for increasing the lift will result in a material improvement of the efficiency of the present-day airplane.

LANGLEY MEMORIAL AERONAUTICAL LABORATORY,
NATIONAL ADVISORY COMMITTEE FOR AERONAUTICS,
LANGLEY FIELD, VA., *January 20, 1927.*

REFERENCES

1. NAGEL, F.: Flügel mit seitlichen Scheiben. "Vorläufige Mitteilungen der Aerodynamischen Versuchsanstalt zu Göttingen," No. 2, July, 1924.
2. REID, E. G.: The Effect of Shielding the Tips of Airfoils. N. A. C. A. Technical Report No. 201, 1925.
3. LAMB, H.: Hydrodynamics—Fifth edition, 1924.
4. PRANDTL, L.: Applications of modern Hydrodynamics to Aeronautics. N. A. C. A. Technical Report No. 116, 1925.
5. HIPPISEY, R. L.: Smithsonian Mathematical Formulae and Tables of Elliptic Functions. Smithsonian Miscellaneous Collections. Volume 74, No. 1, 1922.
6. Tragflügel Theorie, zweite Mitteilung. (Nachrichten der Königlichen Gesellschaft der Wissenschaften zu Göttingen. Mathematische-Physikalische, 1919.)
7. PRANDTL, L.: Induced Drag of Multiplanes. N. A. C. A. Technical Note No. 182, 1924.

TABLE I

Values of R and $2h/b$ for given values of θ . $R = (\text{area of the equivalent air stream of a monoplane}) / (\text{area of the equivalent air stream of a monoplane with end plates})$. $2h/b = (\text{height of end plate}) / (\text{span of wing})$.

θ degrees	$2h/b$	R	Nagel's formula	Per cent difference
15	0.0173	0.971	0.974	+0.33
20	.0311	.948	.951	.32
25	.0493	.909	.925	1.76
30	.0721	.877	.895	2.05
35	.0996	.844	.859	1.78
40	.133	.800	.820	2.50
45	.173	.751	.777	3.47
50	.222	.704	.731	3.83
55	.285	.653	.678	3.80
60	.349	.610	.633	3.77
65	.433	.562	.582	3.56
70	.541	.508	.527	3.74
75	.686	.452	.468	3.15
80	.897	.395	.401	+1.52
85	1.27	.323	.321	-.62
88	1.78	.261	.252	-3.45
89	2.17	.227	.217	-4.40

TABLE II

OBSERVED AND CALCULATED REDUCTION OF DRAG

[Tests made at Langley Memorial Aeronautical Laboratory. Monoplane, 4 by 24 inches; wing section, N. A. C. A. 73]

C_L	C_D (disk end plates)		Difference of observed and calculated reduction as per cent of drag	C_D (trapezoidal end plates)		Difference of observed and calculated reduction as per cent of drag
	Observed	Calculated		Observed	Calculated	
0	-0.0026	-0.00210	+3.90	-0.0010	-0.00113	-0.18
.1	-.0020	-.00196	+.35	-.0007	-.00105	-3.50
.2	-.0013	-.00159	-2.40	-.0007	-.0008	-.83
.3	-.0003	-.00095	-4.60	-.0003	-.00039	-.63
.4	+.0005	-.00005	+3.15	+.00020	-.00018	+.11
.5	+.0012	+.00110	+.95	.0007	+.00092	-1.00
.6	+.0023	+.00250	-.72	+.0016	+.00183	-.82
.7	+.0038	.00412	-.90	+.0027	+.00289	-.54
.8	+.0064	.00604	+.82	+.0036	+.00413	-1.21
.9	+.0093	.00826	+1.82	+.0060	+.00553	+.83
1.0	+.0180	.01060	+8.22	+.0162	+.00708	+10.10